Analytical Design of Wire-Bonded Multiconductor Transmission-Line-Based Ultra-Wideband Differential Bandpass Filters

Juan José Sánchez-Martínez and Enrique Márquez-Segura, *Senior Member, IEEE*

***Abstract*—A systematic design process of ultra-wideband differential bandpass filters based on wire-bonded multiconductor transmission lines is presented. The topology is thoroughly analyzed by means of analytical design equations that provide some insights into the physical behavior of the proposed structure. Single- and double-section configurations are introduced and exact closed-form design equations are derived to design differential filters with either a Butterworth or Chebyhsev frequency response. To validate the design procedure, two differential filters are designed and fabricated with an equal-ripple fractional bandwidth (FBW) of 100% and 60% (3-dB FBW of 145% and 97%), respectively. The measured differential-mode responses show a good in-band flatness with insertion losses lower than 1 dB and with high common-mode rejection levels greater than 20 dB. Experimental results demonstrate a good agreement with theory and prove that the proposed design methodology is useful for accurate and fast ultra-wideband differential filter synthesis.**

***Index Terms*—Bandpass filter, common mode, coupled lines, differential filter, differential mode, multiconductor transmission lines (MTLs), ultra-wideband.**

I. Introduction

TODAY, the use of balanced circuits is increasingly widespread by their benefits over single-ended techniques. The signal processing in differential devices provides high-noise immunity, increased dynamic range, and reduced even-order distortion for differential low-noise amplifiers. In addition, the increase in the dynamic range compared to a similar single-ended circuit implementation is of great interest because it allows reducing the circuit supply voltage, and consequently, the circuit power consumption [1]. In that sense, differential filters with common-mode rejection capability have become essentials in the design of balanced circuits.

Different topologies have been proposed to differential filtering with common-mode suppression. A branch-line structure is proposed in [2], which is extended in [3] by increasing the selectivity. However, the circuit size is enlarged and the achieved differential-mode passband is only of 62%. Another branch-line structure, based on a double-sided parallel-strip line, is introduced in [4], a three-layer broadside coupled microstrip-slot-microstrip structure is used in [5], and a differential wideband bandpass filter using a slot-line resonator is presented in [6]. Notwithstanding, these topologies increase the fabrication complexity and the introduction of the slot-line can cause electromagnetic interference. Coupled-resonator configurations based on stepped-impedance resonators have been proposed in [7] and [8] and recently, an S-shaped complementary split-ring resonator has been employed in [9], but they have a limited bandwidth. Differential filters based on T-shaped structures [10] or with other different topologies have been also explored in [11] and [12]. However, the design of compact ultra-wideband differential passband filters with common-mode suppression is still a challenge.

Coupled-line based differential filters are presented in [13] and [14]. Both works employ similar structures, but in [13], the design of an interdigital filter for the differential passband is proposed, while in [14] only two lines are employed. However, the differential-mode passband in [13] is degraded with return losses of about 5 dB, and filters in [14] are only suitable for narrowband applications. In addition, most of these designs either lack of a systematic design procedure in order to analytically compute the filter design parameters to meet a prescribed frequency response, or are based on approximate techniques for narrow and moderate bandwidths employing ideal impedance or admittance inverters [15].

In this work, a compact differential bandpass filter based on wire-bonded multiconductor transmission lines (MTLs) is proposed and analyzed by means of analytical design equations. Under the odd-mode excitation, the filter can be easily designed to have ultra-wideband differential-mode passband, while it provides a good common-mode rejection for common-mode signals. It can be demonstrated that the differential-to-differential S-parameters of the filter only depends on the design of the odd-mode equivalent circuit. The synthesis procedure, as in [16]–[18], is carried out by computing and equating the transfer functions of the proposed filters to Butterworth or Chebyshev filtering functions. Thus, the theory given in [19] for bandpass filters is extended and generalized to obtain closed-form design formulas. Once the fractional bandwidth (FBW) and required return losses are chosen, the circuit design parameters can be calculated. Several prototypes are synthesized and fabricated to validate the predicted theoretical differential-mode frequency responses.

Manuscript received March 20, 2014; revised June 25, 2014; accepted July 20, 2014. Date of publication August 14, 2014; date of current version October 02, 2014. This work was supported by the Junta de Andalucía under Grant P09-TIC-5116.

The authors are with the Departamento de Ingeniería de Comunicaciones, Escuela Técnica Superior de Ingeniería de Telecomunicación, Universidad de Málaga, 29071 Málaga, Spain (e-mail: jjsm@ic.uma.es, ems@ic.uma.es).

Color versions of one or more of the figures in this paper are available online at http://ieeexplore.ieee.org.

Digital Object Identifier 10.1109/TMTT.2014.2345338

II. Analysis and Design

A wire-bonded MTL is a specific case of MTLs, in which bonding wires interconnect the ends of alternate conductors. Assuming ideal short circuits across alternate conductors, the connections can be neglected and the equivalent-circuit model for a wire-bonded MTL can be reduced to just a pair of coupled lines [20]. As a result, with this simplified configuration, there are now only two independent conductors and the operating bandwidth is increased since undesired resonances are suppressed. The proposed differential filter consists of cascaded two-port short-circuited wire-bonded MTLs [19]. By increasing the number of MTLs, the selectivity of the filter is enhanced, but the large overall size can be a cumbersome issue for practical applications. Taking into account this consideration and pursuing the synthesis of wideband frequency responses, the following analytical study is carried out for single- and double-section filters.

A. Single-Section Differential Filter

For a single-section differential filter, two wire-bonded MTLs are connected as represented in Fig. 1(a). This topology is ideally symmetrical, and thus, it can be readily analyzed under odd- and even-mode excitations. The equivalent half-circuits that result from differential and common mode are sketched in Fig. 1(b) and (c), respectively. The admittance matrices of both circuits can be computed as [19]

$$[Y]_o = \begin{bmatrix} Y_{11_o} & Y_{12_o} \\ Y_{21_o} & Y_{22_o} \end{bmatrix} = \begin{bmatrix} -jM\cot\theta & jN\csc\theta \\ jN\csc\theta & -jM\cot\theta \end{bmatrix} \quad (1a)$$

$$[Y]_e = \begin{bmatrix} Y_{11_e} & Y_{12_e} \\ Y_{21_e} & Y_{22_e} \end{bmatrix} = \begin{bmatrix} -j\frac{M^2-N^2}{M}\cot\theta & 0 \\ 0 & jM\tan\theta \end{bmatrix} \quad (1b)$$

where subscripts o and e stand for the odd- and even-mode circuits, and θ is the electrical length of the conductors. M and N are related to the even- and odd-mode impedances of a pair of coupled lines as [21]

$$M = \frac{1}{Z_{oe}+Z_{oo}}\left(1+\frac{(k-1)}{2}\frac{Z_{oe}^2+Z_{oo}^2}{Z_{oe}Z_{oo}}\right) \quad (2a)$$

$$N = \frac{k-1}{2}\frac{Z_{oo}-Z_{oe}}{Z_{oe}Z_{oo}} \quad (2b)$$

where k is the number of conductors. From (1), it is straightforward to observe that the equivalent circuit under differential excitation has a bandpass frequency response, whereas there is a theoretical perfect rejection of the common mode because $Y_{12_e} = Y_{21_e} = 0$, and thus, common-mode signals are not transmitted [22]. By simple transformations of (1), the mixed-mode S-parameters [1] of the balanced filter are given by

$$[S]^{mm} = \begin{bmatrix} S_{dd_{11}} & S_{dd_{12}} & S_{dc_{11}} & S_{dc_{12}} \\ S_{dd_{21}} & S_{dd_{22}} & S_{dc_{21}} & S_{dc_{22}} \\ S_{cd_{11}} & S_{cd_{12}} & S_{cc_{11}} & S_{cc_{12}} \\ S_{cd_{21}} & S_{cd_{22}} & S_{cc_{21}} & S_{cc_{22}} \end{bmatrix} = \begin{bmatrix} S_{11_o} & S_{21_o} & 0 & 0 \\ S_{21_o} & S_{11_o} & 0 & 0 \\ 0 & 0 & S_{11_e} & 0 \\ 0 & 0 & 0 & S_{22_e} \end{bmatrix}. \quad (3)$$

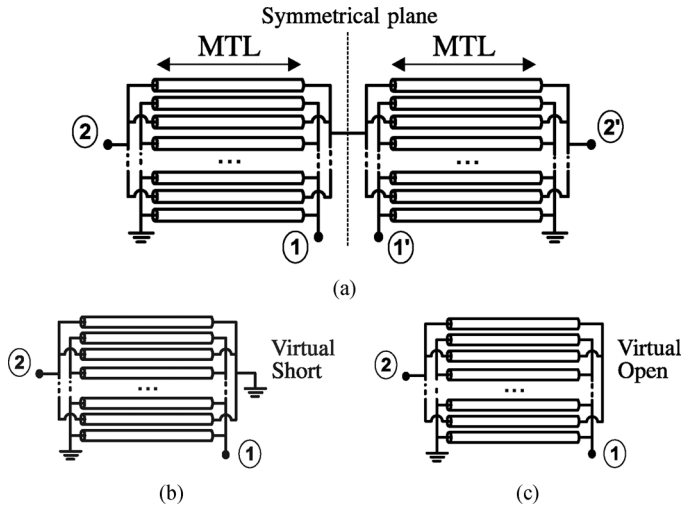

Fig. 1. (a) Transmission-line equivalent-circuit model for a single-section wideband differential bandpass filter and corresponding circuits in: (b) odd- and (c) even-mode excitations.

From (3), it can be seen that the differential-to-differential terms only depend on the design of the odd-mode equivalent circuit. Besides, because the proposed structure is reciprocal and symmetrical, the cross-mode S-parameters are zero [23]. The half-circuit depicted in Fig. 1(b) was introduced in [19] to design wide-bandpass filters with left-handed behavior, but expressions deduced in that work are complex and not suited for designing a filter with desired particular return losses and operating bandwidth.

The frequency response of the proposed filter can be inferred from the image impedance [24] of the odd-mode equivalent circuit. From (1), the image impedance of the two-port short-circuited wire-bonded MTL [see Fig. 1(b)] is computed as

$$Z_I = Z_c\frac{c\sin\theta}{\sqrt{c^2-\cos^2\theta}} \quad (4)$$

where Z_c and c are defined as [25]

$$Z_c = \frac{-1}{N} \quad c = \frac{-N}{M}. \quad (5)$$

c is related to the maximum coupling coefficient of a k-line quarter-wavelength four-port coupler [21], and considering (4), it is clear that the image impedance of the two-port circuit is equal to the characteristic impedance Z_c at $\theta = \pi/2$ that normally corresponds to the design center frequency. Besides, as will be demonstrated later, the value of Z_c determines the type of wideband frequency response (Butterworth or Chebyshev response).

Fig. 2 depicts the image impedance, normalized by Z_c for several values of c. As seen, there is a frequency range where the image impedance is purely real, but outside of this band it behaves as a capacitive reactance. In addition, from this figure, it is possible to deduce two main properties of the structure. First, by increasing the coupling c, the frequency range with purely real image impedance values is broadened. Thus, as it is well known in coupled-line filters [26], the greater the coupling factor, the wider the operating bandwidth. Second, as Z_0 is the characteristic impedance used to terminate the input and

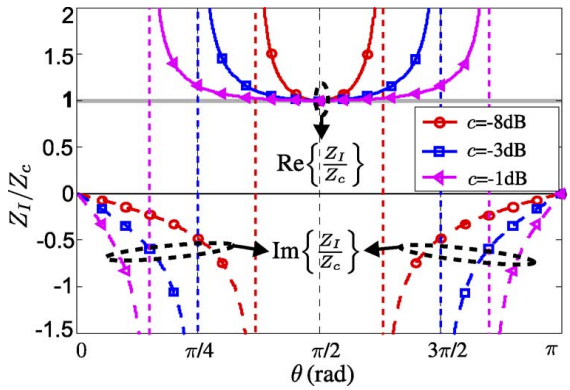

Fig. 2. Image impedance of a two-port short-circuited wire-bonded MTL [odd-mode equivalent circuit, Fig. 1(b)] normalized by its characteristic impedance Z_c for several coupling values (5).

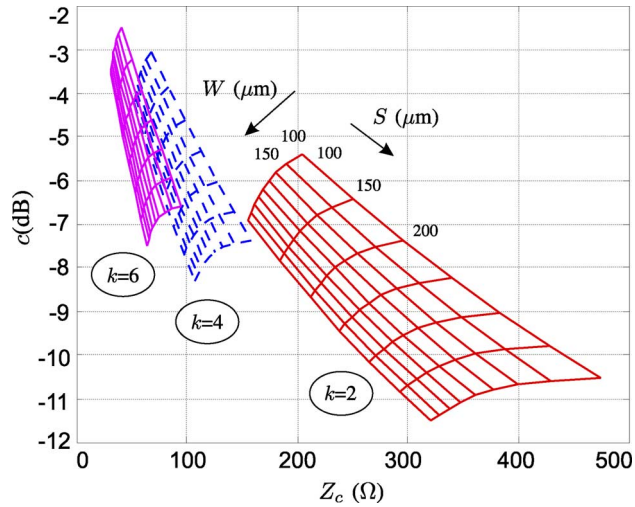

Fig. 3. Characteristic impedance Z_c and coupling factor c for a two-port short-circuited wire-bonded as a function of the width W and spacing S for several number of conductors k (R04350B substrate with a dielectric constant of 3.66 and thickness of 30 mil, grid spacing $= 50$ μm).

output ports, the filter can be designed to have either a Butterworth or a Chebyshev response with two transmission poles. If $Z_c = Z_0$, the wire-bonded MTL is matched at $\theta = \pi/2$, regardless of the coupling factor c, and for values of $Z_c < Z_0$, there are two frequencies with perfect matching. Therefore, if the MTL is a quarter-wavelength long at the design frequency, it can be readily designed to be matched at midband frequency for a maximally flat response ($Z_c = Z_0$) or to have an equal-ripple response with two transmission poles ($Z_c < Z_0$).

It is important to highlight that, in this work, the MTLs are synthesized to achieve a prescribed frequency response. The design equations to calculate Z_c and c (5) will be different to the design equations for a k-line coupler [21]. In a four-port directional coupler, a condition for perfect match and perfect isolation [$Z_c^2 = 1/(M^2 - N^2)$] is imposed, while in this work, the characteristic impedance Z_c and c are related to the desired frequency response. Therefore, c must be interpreted as a design variable and not as the coupling factor of a directional coupler. This property is useful for designers because the fabrication complexity of the structure is not only conditioned by the value of c, but also by Z_c. Such behavior is shown in Fig. 3, where the achievable values of c and Z_c are represented as a function of the line width W and spacing S for several number of conductors k. The substrate chosen, which will be used throughout this work, is Rogers 4350B, with a dielectric constant of 3.66 and thickness of 30 mil. In particular, from Fig. 3 and taking into account the tendency of curves, it is remarkable that it is difficult to obtain low values of Z_c with high coupling levels with only two conductors. This is remarkable because in order to design a two-pole wideband bandpass filter, it is necessary to achieve high values of c with values of Z_c lower than the load impedance Z_0. Therefore, the importance of increasing the number of conductors for designing wideband differential filters using short-circuited wire-bonded MTLs is demonstrated.

The use of the image impedance enhances the physical insight into the frequency behavior of the structure. However, it should be worth obtaining a set of design expressions for synthesizing a desired frequency response. In that case, the design procedure using the insertion-loss method is more expedient [24] to find a direct relation between the filter performance (operating bandwidth and return loss) and the design variables Z_c and c.

From (1a), the differential S-parameters are computed by applying the following transformations:

$$S_{dd_{11}} = S_{dd_{22}} = \frac{Y_0^2 - Y_{11_o}^2 + Y_{12_o}^2}{(Y_0 + Y_{11_o})^2 - Y_{12_o}^2} \tag{6a}$$

$$S_{dd_{12}} = S_{dd_{21}} = \frac{-2Y_{12_o}Y_0}{(Y_0 + Y_{11_o})^2 - Y_{12_o}^2} \tag{6b}$$

with $Y_0 = 1/Z_0$. Using (6), the differential terms are expressed as

$$S_{dd_{11}} = \frac{c^2\left(\bar{Z}_c^2 \sin^2\theta - 1\right) + \cos^2\theta}{c^2\left(\bar{Z}_c^2 \sin^2\theta + 1\right) - \cos^2\theta - j2c\bar{Z}_c \cos\theta \sin\theta} \tag{7a}$$

$$S_{dd_{21}} = \frac{j2c^2\bar{Z}_c \sin\theta}{c^2\left(\bar{Z}_c^2 \sin^2\theta + 1\right) - \cos^2\theta - j2c\bar{Z}_c \cos\theta \sin\theta} \tag{7b}$$

where $\bar{Z}_c = Z_c/Z_0$. Thus, $\bar{Z}_c$ stands for the impedance Z_c (5) of the short-circuited MTL normalized by the reference impedance Z_0. In addition, the square of the modulus of these transmission and reflection terms can be written as

$$|S_{dd_{21}}|^2 = \frac{1}{1 + F_I^2} \quad |S_{dd_{11}}|^2 = 1 - |S_{dd_{21}}|^2 \tag{8}$$

with

$$F_I = \frac{1 - c^2\bar{Z}_c^2}{2c^2\bar{Z}_c}\left(\cos^2\theta + \frac{c^2(\bar{Z}_c^2 - 1)}{1 - c^2\bar{Z}_c^2}\right)\frac{1}{\sin\theta} \tag{9}$$

and where a lossless system is considered. F_I is a second-order polynomial that determines the filtering properties of the structure. From filter theory, it is straightforward to calculate F_I in order to conform the transfer function as follows:

$$\varepsilon F_n = F_I \tag{10}$$

where F_n is an nth-order Butterworth or Chebyshev polynomial (second order for this configuration) and ε is the in-band ripple factor, related to the return losses L_R as [27]

$$\varepsilon = \frac{1}{\sqrt{10^{L_R/10}-1}}. \tag{11}$$

Thus, the design of the filter consists of finding the values of c and Z_c to meet the requirements of bandwidth and return losses. The FBW of the filter is defined by

$$\mathrm{FBW} = \frac{f_2 - f_1}{f_o} \tag{12}$$

where f_1 and f_2 are the passband limits of the filter, and f_o is the design frequency. Assuming a TEM propagation and that the wire-bonded MTL is a quarter-wavelength long at the design frequency, the electrical length of the circuit at f_1 is calculated as

$$\theta_{c1} = \frac{\pi}{2}\left(1 - \frac{\mathrm{FBW}}{2}\right). \tag{13}$$

For Butterworth responses, f_1 and f_2 are the -3-dB points of the bandpass ($L_R = 3$ dB), whereas for Chebyshev filters, both frequencies determine the bandwidth with equal-ripple level (11).

Therefore, given the operating bandwidth and the return losses, the following two design equations are found:

$$\text{Butterworth} = \begin{cases} \bar{Z}_c = 1 \\ c = \frac{1}{\sqrt{1+2\varepsilon\tan\theta_{c1}\sec\theta_{c1}}} \end{cases} \tag{14a}$$

$$\text{Chebyshev} = \begin{cases} \bar{Z}_c = -\varepsilon + \sqrt{\varepsilon^2+1} \\ c = \frac{\cos\theta_{c1}}{\sqrt{2+\bar{Z}_c^2\left(\cos\theta_{c1}^2-2\right)}} \end{cases} \tag{14b}$$

where θ_{c1} is related to the FBW by means of (13). It is important to mention that the design formula for the Butterworth response is exact, but for the Chebyshev response, it is an approximation because the polynomial F_I is not a standard second-order Chebyshev polynomial. The effect of this approximation is shown in Fig. 4, where the achieved bandwidths (FBW^*), calculated using (8) and the relative error (Δ_{FBW}) are depicted as a function of the design FBWs. As seen, the error grows with the desired bandwidth, but considering its magnitude, lower than 12% for an FBW of 120%, it can be deduced that the design (14b) provides a good result. Notwithstanding, the deviation from the design values can be accurately estimated using the following formulas, which have been obtained by curve fitting:

$$\Delta_{\mathrm{FBW}}(\%) = 10^{-3}\left[0.872\,\mathrm{FBW}^2 - 10.59\,\mathrm{FBW} + 355.2\right] \tag{15a}$$

$$\mathrm{FBW} = 10^{-3}\left[3.477(\mathrm{FBW}^*)^2 + 710.9\,\mathrm{FBW}^* + 6054\right]. \tag{15b}$$

Therefore, to get a reliable synthesis process of wideband Chebyshev filters (14b), and FBW^* being the final achieved bandwidths, the initial design FBW used to compute θ_{c1} (13) may be adjusted according to (15b). The error committed after that correction is represented in Fig. 4. As seen, this correction should only be applied for bandwidths greater than 40% in order to maintain the relative error lower than 2%.

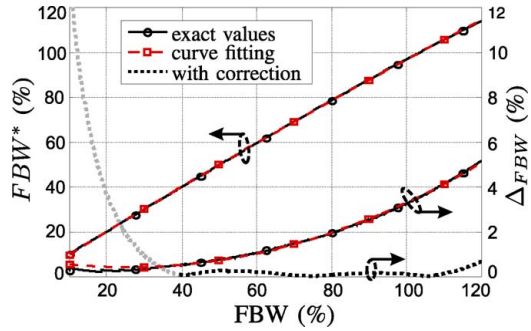

Fig. 4. Achieved FBWs (FBW^*) for a single-section differential filter, calculated using (8), and relative error Δ_{FBW} with respect to the design FBWs of Chebyshev filters, before and after the correction given by (15b).

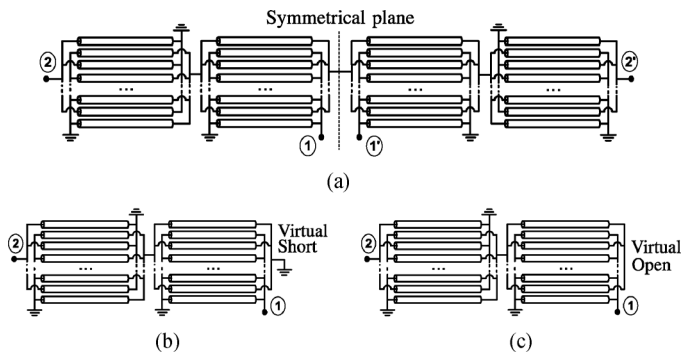

Fig. 5. (a) Transmission-line equivalent-circuit model for a two-section wideband differential bandpass filter and corresponding circuits in: (b) odd- and (c) even-mode excitations.

B. Double-Section Differential Filter

The proposed configuration analyzed in Section II-A is straightforward to design ultra-wideband differential filters with good common-mode rejection. However, to increase the selectivity, double-section bandpass filters are introduced and investigated. The new topology, depicted in Fig. 5(a), can be bisected into two identical halves with respect to its symmetrical interface. Fig. 5(b) and (c) shows the two bisections under differential- and common-mode operation, respectively. Considering these two half networks, it is seen that the odd-mode circuit has a bandpass frequency response, whereas the even-mode half circuit rejects the common-mode signals [22].

The design of the double-section differential filter is carried out analyzing the odd-mode circuit. By using the admittance matrix (1b), the square of the magnitude of the S-parameters can be found as

$$|S_{dd_{21}}|^2 = \frac{1}{1+F_{II}^2} \quad |S_{dd_{11}}|^2 = 1 - |S_{dd_{21}}|^2 \tag{16}$$

where

$$F_{II} = \frac{1-c^2\bar{Z}_c^2}{c^3\bar{Z}_c}\cos\theta\left(\cos^2\theta + \frac{c^2(\bar{Z}_c^2-1)}{1-c^2\bar{Z}_c^2}\right)\frac{1}{\sin\theta}. \tag{17}$$

F_{II} is a third-order polynomial that conditions the transfer function of the filter. In a similar way to the previous synthesis process, by properly designing F_{II} (10), the filtering transfer

function can be designed as a Butterworth or a Chebyshev response. In addition, as the order of F_{II} is increased, the skirt selectivity of the filter is enhanced, and some new design equations are required to find the values of c and Z_c that satisfy a particular frequency response.

From (16) and (17), the following closed-form design equations are deduced [28].

- Butterworth, $\bar{Z}_c = 1$,

$$G = \varepsilon \tan\theta_{c1}\left(1+\tan^2\theta_{c1}\right) \tag{18a}$$

$$R = \frac{1}{2G} - \frac{1}{27G^3} \quad Q = -\frac{1}{9G^2} \tag{18b}$$

$$S_1 = \sqrt[3]{R+\sqrt{Q^3+R^2}} \quad S_2 = \sqrt[3]{R-\sqrt{Q^3+R^2}} \tag{18c}$$

$$c = S_1 + S_2 - \frac{1}{3G}. \tag{18d}$$

- Chebyshev,

$$r = \frac{\varepsilon\left(\varepsilon^2-\cos^2\theta_{c1}+2\right)}{\cos^3\theta_{c1}} \tag{19a}$$

$$g = \sqrt{\frac{3\varepsilon^2[6\cos^4\theta_{c1}-(27\varepsilon^2+36)\cos^2\theta_{c1}+36(1+\varepsilon^2)]-\cos^6\theta_{c1}}{27\cos^6\theta_{c1}}} \tag{19b}$$

$$S_1 = \sqrt[3]{r+g} \quad S_2 = \sqrt[3]{r-g} \tag{19c}$$

$$u = S_1 + S_2 + \frac{\varepsilon}{\cos\theta_{c1}} \tag{19d}$$

$$c = \sqrt{\frac{\cos^3\theta_{c1}(u^2-1)}{4u\varepsilon}} \tag{19e}$$

$$\bar{Z}_c = \frac{1}{\sqrt{1+\frac{3}{4}(u^2-1)\cos^2\theta_{c1}}} \tag{19f}$$

where θ_{c1} is related to the desired FBW by means of (13). For Butterworth response L_R is normally equal to 3 dB, and thus, $\varepsilon = 1$.

By using (18) and (19), a third-order Butterworth response or a three-pole Chebyshev filter with equal ripple can be readily designed. In addition, as in the previous discussion, the solution for Butterworth filters is exact, but the design (19e) and (19f) provide approximated solutions because F_{II} is not a standard third-order Chebyshev polynomial. Fig. 6 depicts the difference between the desired FBWs and the actually obtained FBW* by evaluating (16). The relative error shows that the maximum error is always lower than 6% for bandwidths up to 120%. Thus, the design equations for Chebyshev filters provide very good results. Nevertheless, as in Section II-A, both the deviation from the expected FBW and the relative error committed, can be computed using the following formulas obtained by curve fitting:

$$\Delta_{\mathrm{FBW}}(\%) = 10^{-3}\left[0.522\,\mathrm{FBW}^2 - 26.81\,\mathrm{FBW} + 751.7\right] \tag{20a}$$

$$\mathrm{FBW} = 10^{-3}\left[1.11(\mathrm{FBW}^*)^2 + 904.5\,\mathrm{FBW}^* + 2256\right]. \tag{20b}$$

Therefore, to improve the precision, the design FBW may be modified according to (20b). As depicted in Fig. 6, by making this correction for operating bandwidths greater than 40%, the relative error is always below 1%.

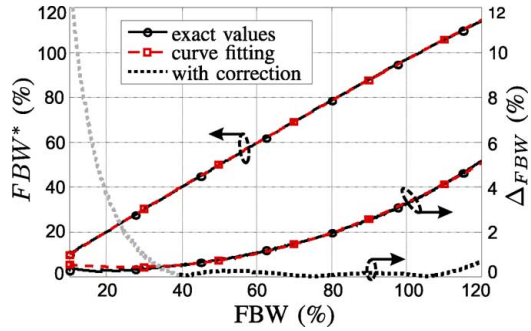

Fig. 6. Achieved FBWs (FBW*) for a two-section differential filter, calculated using (16), and relative error Δ_{FBW} with respect to the design FBWs of Chebyshev filters, before and after the correction given by (20b).

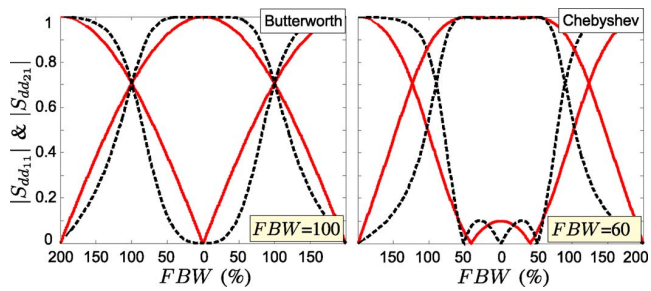

Fig. 7. Magnitude of the theoretical $S_{dd_{11}}$ and $S_{dd_{21}}$ for a single-section (solid line) and double-section filter (dashed line) designed with a Buterworth or Chebyshev function response ($L_R = 20$ dB).

TABLE I
DESIGN PARAMETERS OF FILTERS DEPICTED IN FIG. 7

	Butterworth			Chebyshev (LR=-20dB)		
	FBW	c	Z_c	FBW	c	Z_c
single-section	100	-4.78	50	60	-4.12	45.23
double-section	100	-3.65	50	60	-4.45	41.03

To compare the performance of both single- and double-section differential filters, Fig. 7 represents the magnitude of the calculated $S_{dd_{11}}$ and $S_{dd_{21}}$ for two Butterworth and Chebyshev filters. For the Butterworth response, a 3-dB FBW of 100% is used, while for the Chebyshev type, an equal-ripple FBW of 60% is selected. The design of these filters is carried out by means of (14a) and (18) for the Buttherworth response, and (14b) and (19) with $L_R = 20$ dB for the Chebyshev function. From these curves, it can be deduced that the Chebyshev response, with two or three transmission poles, is more suitable to achieve wideband bandpass filters with a good selectivity. The design parameters obtained for each filter are listed in Table I.

The theory presented in Sections II-A and II-B allows the values of c and Z_c to be computed in order to obtain a desired frequency response taking into account both the FBW and the return losses. Once these values are known by means of either design formula (14a), (14b), (18), or (19), the required even- and odd-mode impedances can be calculated, from (5) and (2b), as

$$Z_{oe} = \frac{k-1}{2}Z_c(R-1) \quad Z_{oo} = \frac{Z_{oe}}{R} \tag{21a}$$

$$R = \frac{c+\sqrt{(k-1)^2(1-c^2)+c^2}}{(k-1)(1-c)}. \tag{21b}$$

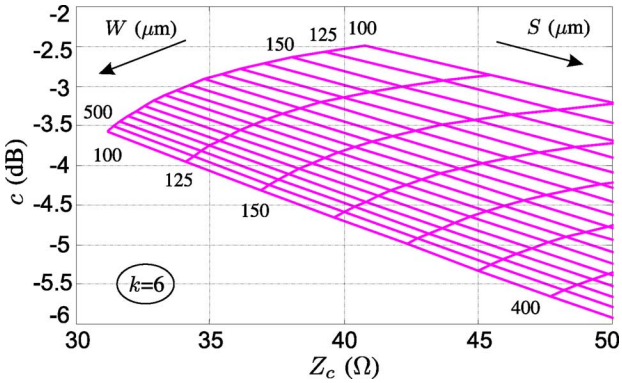

Fig. 8. Line width W and spacing S of a two-port short-circuited wire-bonded in order to achieve values of characteristic impedance $Z_c \leq 50\ \Omega$.

TABLE II
DESIGN PARAMETERS AND PHYSICAL DIMENSIONS OF THE FABRICATED CHEBYSHEV DIFFERENTIAL FILTERS

	FBW (%)	L_R (dB)	c (dB)	Z_c (Ω)	k	W (μm)	S (μm)	d (mm)
single-section	100	-15	-3.47	44	6	110	110	13.6
double-section	60	-25	-2.67	42	6	190	150	13.8

FBW: Fractional bandwidth with equal-ripple response

III. EXPERIMENTAL VALIDATION

In this section, several prototypes of the proposed differential filter are designed and manufactured in order to validate the presented analytical design process. The dielectric substrate used is Rogers 4350B having a dielectric constant of 3.66 and thickness of 30 mil (the same substrate employed in Section II). From theory, it was demonstrated that a value of $Z_c \leq 50\ \Omega$ is required to synthesize wideband Butterworth- or Chebyshev-type responses. In that sense, Fig. 8 depicts the allowed physical dimensions of a wire-bonded MTL to obtain useful values of Z_c (5). As seen, for the selected substrate, only if $k = 6$ the value of Z_c is less than 50 Ω. Therefore, from Fig. 8, it is possible to highlight the importance of using more than two conductors in designing wideband differential filters (see Fig. 3). In this work, the minimum line width and spacing is limited to 100 μm according to our fabrication capability.

Taking into account the above considerations, one two-pole (single section) and one three-pole (double section) Chebyshev differential filters are designed for a midband frequency $f_o = 3.5$ GHz. The theoretical operating bandwidth, return losses, and the physical dimensions of both filters are collected in Table II. The design values c and Z_c are easily computed by means of (14b) and (19) for the two- and three-pole filters, respectively. Once these values are known, the required even- and odd-mode impedances as a function of the number of conductors k are calculated (21) and then translated into physical dimensions [29], [30].

Fig. 9 depicts the wideband differential- and common-mode theoretical, simulated, and measured responses of the fabricated filters. Ansys HFSS v15 is used to simulate both prototypes, while the measured responses are obtained by using a dual-source four-port vector network analyzer (Agilent N5247A PNA-X) in order to apply true-differential or true-common-mode stimulus in both forward and reverse directions. The photographs of these two- and three-pole filters are shown in Fig. 9(a) and (b), respectively.

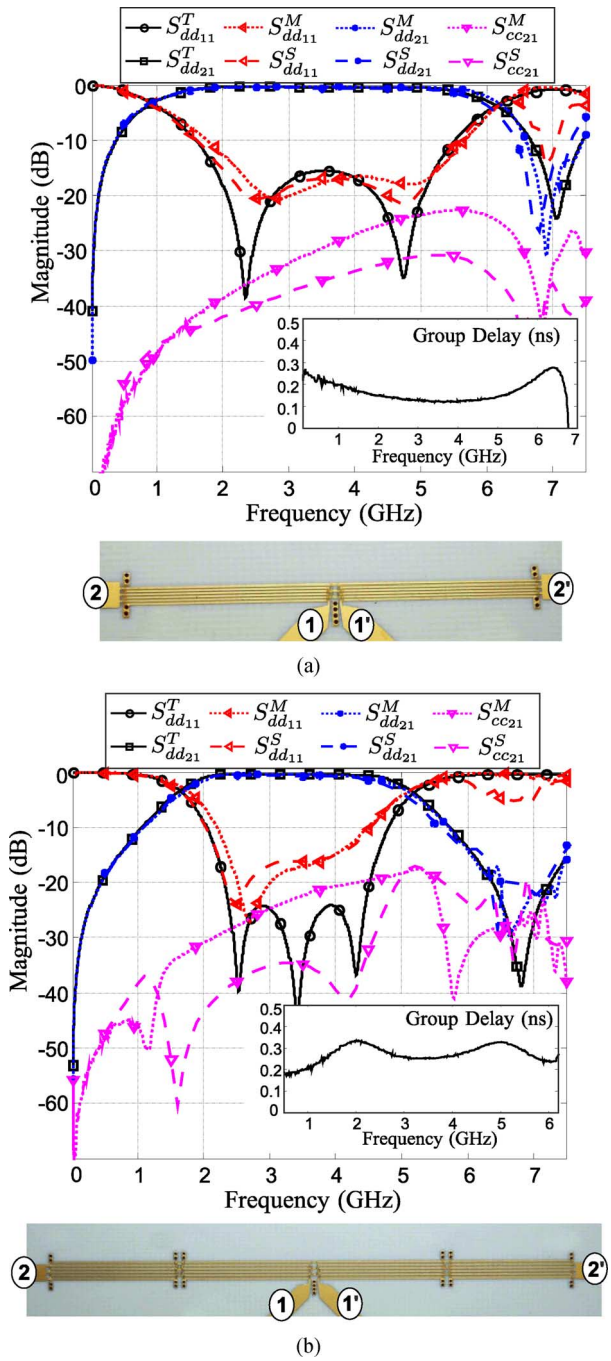

Fig. 9. Wideband differential- and common-mode theoretical (T), simulated (S), and measured (M) responses of the fabricated filters.

From Fig. 9, it is noted that there is a good agreement between the measurements and the predicted results by using the analytical formulas derived in this work. There is an excellent concordance between the theoretical and measured differential insertion losses ($S_{dd_{21}}$), but there are some discrepancies in the differential-mode return losses ($S_{dd_{11}}$). It is important to remark that both filters have been fabricated by directly using the computed theoretical values without any optimization during

the electromagnetic simulations. This fact is important because the goal of this work is not only to prove the feasibility of designing wideband differential filters, but also the validity of the presented theory. In that sense, the new design equations are valuable to design differential bandpass filters with a desired operating bandwidth with great exactitude. The measured insertion losses are lower than 1 dB within the designed differential passband, and the 3-dB FBWs extends up to 145% and 97% for the single- and double-section filters, respectively. In addition, the common-mode rejection level ($S_{cc_{21}}$) is better than 20 dB in both prototypes and the measured group delay (see Fig. 9) is below 0.4 ns, indicating a good phase linearity.

It is important to mention that the reduction on the common-mode rejection capability (in both simulated and measured responses) and the discrepancies in the return loss are mainly due to the difference between the even- and odd-mode phase velocities in the wire-bonded MTL. This effect is well known, and it can be mitigated by equalizing both phase velocities [20]. Notwithstanding, even without this compensation, the closed-form design equations derived in this work are useful to synthesize wideband differential filters with a prescribed operating bandwidth.

IV. Conclusion

In this paper, a structure consisting of short-circuited wire-bonded MTLs has been analyzed to design ultra-wideband differential filters with a good common-mode rejection. A set of new design equations has been presented to synthesize filters with a Butterworth- or Chebyshev-type response by means of a quick and reliable procedure. These analytical equations allow designers to compute the required even- and odd-mode impedances of the wire-bonded MTLs in order to obtain a desired frequency response. Expressions for two configurations, single- and double-section filters, have been deduced and validated by means of experimental results.

References

[1] W. R. Eisenstadt, B. Stengel, and B. M. Thompson, *Microwave Differential Circuit Design Using Mixed-Mode S-Parameters*. Norwood, MA, USA: Artech House, 2006.

[2] T. B. Lim and L. Zhu, "A differential-mode wideband bandpass filter on microstrip line for UWB application," *IEEE Microw. Wireless Compon. Lett.*, vol. 19, no. 10, pp. 632–634, Oct. 2009.

[3] T. Lim and L. Zhu, "Differential-mode ultra-wideband bandpass filter on microstrip line," *Electron. Lett.*, vol. 45, no. 22, pp. 1124–1125, Oct. 2009.

[4] X.-H. Wang, Q. Xue, and W.-W. Choi, "A novel ultra-wideband differential filter based on double-sided parallel-strip line," *IEEE Microw. Wireless Compon. Lett.*, vol. 20, no. 8, pp. 471–473, Aug. 2010.

[5] A. Abbosh, "Ultrawideband balanced bandpass filter," *IEEE Microw. Wireless Compon. Lett.*, vol. 21, no. 9, pp. 480–482, Sep. 2011.

[6] Y.-J. Lu, S.-Y. Chen, and P. Hsu, "A differential-mode wideband bandpass filter with enhanced common-mode suppression using slotline resonator," *IEEE Microw. Wireless Compon. Lett.*, vol. 22, no. 10, pp. 503–505, Oct. 2012.

[7] C.-H. Wu, C.-H. Wang, and C. H. Chen, "Balanced coupled-resonator bandpass filters using multisection resonators for common-mode suppression and stopband extension," *IEEE Trans. Microw. Theory Techn.*, vol. 55, no. 8, pp. 1756–1763, Aug. 2007.

[8] J. Shi and Q. Xue, "Novel balanced dual-band bandpass filter using coupled stepped-impedance resonators," *IEEE Microw. Wireless Compon. Lett.*, vol. 20, no. 1, pp. 19–21, Jan. 2010.

[9] A. Horestani, M. Duran-Sindreu, J. Naqui, C. Fumeaux, and F. Martin, "S-shaped complementary split ring resonators and their application to compact differential bandpass filters with common-mode suppression," *IEEE Microw. Wireless Compon. Lett.*, vol. 24, no. 3, pp. 149–151, Mar. 2014.

[10] W. Feng and W. Che, "Novel wideband differential bandpass filters based on T-shaped structure," *IEEE Trans. Microw. Theory Techn.*, vol. 60, no. 6, pp. 1560–1568, Jun. 2012.

[11] X.-H. Wu and Q.-X. Chu, "Compact differential ultra-wideband bandpass filter with common-mode suppression," *IEEE Microw. Wireless Compon. Lett.*, vol. 22, no. 9, pp. 456–458, Sep. 2012.

[12] W. J. Feng, W. Q. Che, Y. M. Chang, S. Y. Shi, and Q. Xue, "High selectivity fifth-order wideband bandpass filters with multiple transmission zeros based on transversal signal-interaction concepts," *IEEE Trans. Microw. Theory Techn.*, vol. 61, no. 1, pp. 89–97, Jan. 2013.

[13] W. Fathelbab and M. Steer, "Four-port microwave networks with intrinsic broadband suppression of common-mode signals," *IEEE Trans. Microw. Theory Techn.*, vol. 53, no. 5, pp. 1569–1575, May 2005.

[14] C.-H. Wu, C.-H. Wang, and C. H. Chen, "Novel balanced coupled-line bandpass filters with common-mode noise suppression," *IEEE Trans. Microw. Theory Techn.*, vol. 55, no. 2, pp. 287–295, Feb. 2007.

[15] G. L. Mattahei, L. Young, and E. M. T. Jones, *Microwave Filters, Impedance-Matching Networks, and Coupling Structures*. Norwood, MA, USA: Artech House, 1985.

[16] R. Li, S. Sun, and L. Zhu, "Synthesis design of ultra-wideband bandpass filters with composite series and shunt stubs," *IEEE Microw. Wireless Compon. Lett.*, vol. 57, no. 3, pp. 684–692, Mar. 2009.

[17] J.-Y. Li, C.-H. Chi, and C.-Y. Chang, "Synthesis and design of generalized Chebyshev wideband hybrid ring based bandpass filters with a controllable transmission zero pair," *IEEE Trans. Microw. Theory Techn.*, vol. 58, no. 12, pp. 3720–3731, Dec. 2010.

[18] R. Zhang and L. Zhu, "Synthesis design of a wideband bandpass filter with inductively coupled short-circuited multi-mode resonator," *IEEE Trans. Microw. Theory Techn.*, vol. 22, no. 10, pp. 509–511, Oct. 2012.

[19] J. J. Sánchez-Martínez and E. Márquez-Segura, "Analytical study of wideband bandpass filters based on wire-bonded multiconductor transmission lines with LH behaviour," *Progr. Electromagn. Res. Lett.*, vol. 31, pp. 1–13, 2012.

[20] R. Mongia, I. Bahl, and P. Bhartia, *RF and Microwave Coupled-Line Circuits*. Norwood, MA, USA: Artech House, 1999.

[21] W. Ou, "Design equations for an interdigitated directional coupler," *IEEE Trans. Microw. Theory Techn.*, vol. MTT-23, no. 2, pp. 253–255, Feb. 1975.

[22] E. M. T. Jones and J. T. Bolljahn, "Coupled-strip-transmission-line filters and directional couplers," *IRE Trans. Microw. Theory Techn.*, vol. MTT-4, no. 2, pp. 75–81, Apr. 1956.

[23] D. Bockelman and W. Eisenstadt, "Combined differential and common-mode scattering parameters: Theory and simulation," *IEEE Trans. Microw. Theory Techn.*, vol. 43, no. 7, pp. 1530–1539, Jul. 1995.

[24] D. Pozar, *Microwave Engineering*, 2nd ed. New York, NY, USA: Wiley, 1998.

[25] J. J. Sánchez-Martínez and E. Márquez-Segura, "Analysis of wire-bonded multiconductor transmission line-based phase-shifting sections," *J. Electromagn. Waves Appl.*, vol. 27, no. 16, pp. 1997–2009, Sep. 2013.

[26] J.-S. Hong, *Microstrip Filters for RF/Microwave Applications*, K. Chang, Ed. New York, NY, USA: Wiley, 2011.

[27] J.-S. Hong and M. J. Lancaster, *Microstrip Filters for RF/Microwave Applications*, K. Chang, Ed. New York, NY, USA: Wiley, 2001.

[28] M. Abramowitz and I. Stegun, *Handbook of Mathematical Functions with Formulas, Graphs, and Mathematical Tables*. Washington, DC, USA: US Gov. Printing Office, 1972.

[29] M. Kirschning and R. Jansen, "Accurate wide-range design equations for the frequency-dependent characteristic of parallel coupled microstrip lines," *IEEE Trans. Microw. Theory Techn.*, vol. MTT-32, no. 1, pp. 83–90, Jan. 1984.

[30] J. A. B. Faria, "Kirschning and Jansen computer-aided design formulae for the analysis of parallel coupled lines," *Microw. Opt. Technol. Lett.*, vol. 51, no. 10, pp. 2466–2470, 2009.

Juan José Sánchez-Martínez received the B.S., M.S., and Ph.D. degrees in telecommunication engineering from the University of Málaga, Málaga, Spain, in 2003, 2006 and 2014, respectively.

Since March 2006, he has been a Research Assistant with the Department of Communication Engineering, University of Málaga. He was involved in signal processing for digital communications and real-time implementation of signal-processing algorithms on field-programmable gate array until 2010. From May to August 2012, he was a Visiting Scholar with the Department of Electrical and Electronic Engineering, Imperial College London, London, U.K. His current research is focused on the analysis of planar structures and the design of microwave passive devices.

Mr. Sánchez-Martínez was the recipient of a Junta de Andalucía Scholarship (2010–2014).

Enrique Márquez-Segura (S'93–M'95–SM'06) was born in Málaga, Spain, in April 1970. He received the Ingeniero de Telecomunicación and Doctor Ingeniero degrees from the Universidad de Málaga, Málaga, Spain, in 1993 and 1998, respectively.

In 1994, he joined the Departamento de Ingeniería de Comunicaciones, Escuela Técnica Superior de Ingeniería (ETSI) de Telecomunicación, Universidad de Málaga, where, in 2001, he became an Associate Professor. His current research interests include electromagnetic material characterization, measurement techniques, and RF and microwave circuits design for communication applications.

Dr. Márquez-Segura was the recipient of a Spanish Ministry of Education and Science Scholarship (1994–1995).